

quantify the effect. Should such shapes continue to improve the interchange stability, then a study of additional aspects of non-circular RFPs would be warranted, such as ballooning modes localized in regions of local bad curvature, neoclassical effects arising from the strong poloidal asymmetry, and relaxation processes in non-circular plasmas.

#### ACKNOWLEDGEMENT

This work has been supported by the United States Department of Energy, under Grant No. DE-FG02-85ER53212.

#### REFERENCES

- [1] TAMANO, T., BARD, W.D., CARLSTROM, T.N., et al., in Plasma Physics and Controlled Nuclear Fusion Research 1984 (Proc. 10th Int. Conf. London, 1984), Vol. 2, IAEA, Vienna (1985) 431.
- [2] La HAYE, R.J., JENSEN, T.H., LEE, P.S.C., MOORE, R.W., OHKAWA, T., Nucl. Fusion **26** (1986) 255.
- [3] ALMAGRI, A., ASSADI, S., DEXTER, R.N., PRAGER, S.C., SARFF, J.S., SPROTT, J.C., Nucl. Fusion **27** (1987) 1795.
- [4] Various groups of authors, in Plasma Physics and Controlled Nuclear Fusion Research 1984 (Proc. 10th Int. Conf. London, 1984), Vol. 2, IAEA, Vienna (1985) 431, 439, 449, 475, 487.
- [5] GREENE, J.M., JOHNSON, J.L., Phys. Fluids **5** (1962) 510.
- [6] DeLUCIA, J., JARDIN, S.C., TODD, A.M.M., J. Comput. Phys. **37** (1980) 183.
- [7] GREENE, J.M., JOHNSON, J.L., Plasma Phys. **10** (1968) 729.

(Manuscript received 28 August 1987  
Final manuscript received 22 October 1987)

#### MAGNETIC FIELD FLUCTUATIONS IN RIPPLE REDUCTION EXPERIMENTS ON THE REPUTE-1 RFP

K. HATTORI, K. ITAMI, T. FUJITA,  
J. MORIKAWA, H. NIHEI, Z. YOSHIDA,  
N. INOUE (Department of Nuclear Engineering,  
Faculty of Engineering, University of Tokyo,  
Tokyo, Japan), H. JI, A. FUJISAWA,  
N. ASAKURA, K. YAMAGISHI,  
T. SHINOHARA, Y. NAGAYAMA, H. TOYAMA,  
K. MIYAMOTO (Department of Physics, Faculty of  
Science, University of Tokyo, Tokyo, Japan)

**ABSTRACT.** The loop voltage of REPUTE-1 RFP is decreased by reducing the toroidal field ripple. The low frequency part of the toroidal field fluctuations, which is mainly composed of the  $m = 1$  mode and has good coherence in space and time, is found to be reduced, especially outside the reversal surface, when a trimming field is applied. High frequency fluctuations, which have little coherence, are not influenced effectively.

#### 1. INTRODUCTION

The reversed field pinch (RFP) is one of a number of promising magnetic confinement devices [1] which can operate with a relatively small external magnetic

field. One of the key issues of RFP research is the error field problem. It is widely known [2-7] that a small field error degrades the confinement of an RFP plasma and also reduces discharge duration. We should, therefore, decrease the field errors as much as possible and clarify the relationship between field errors and plasma confinement. The effect of field errors arising from port holes and shell gaps has been studied experimentally on ZT-40M [2]. Howell and Vogel [3] have analysed the deviations of magnetic field lines due to port holes. The effect of liner currents on the stability has been studied by Miller [4] on the basis of non-linear tearing mode theory. On HBTX1A [6] and TPE-1R15 [7], it has been shown that cancelling the field error due to the shell gap is important for controlling the equilibrium. Concerning the toroidal field ripple, there is a theoretical estimate of the  $m = 0$  tearing mode stability by Pinsker and Reiman [5].

This paper reports experimental results on ripple reduction for the toroidal field of the REPUTE-1 RFP. The reduction of the toroidal field ripple has been shown to cause a decrease in the loop voltage of the RFP plasma. In addition, magnetic probe measurements have shown that MHD activity (possibly the  $m = 1$  kink mode) has been suppressed by application of the ripple reduction field. In Section 2, we describe the conditions of the present experiment. Section 3 presents the

LETTERS

results of the toroidal ripple reduction experiment from two points of view, i.e. global parameters and magnetic field fluctuations.

2. EXPERIMENTAL SET-UP

The major and minor radii of the liner of the REPUTE-1 RFP [8] are  $R = 82$  cm and  $a = 22$  cm, respectively. The minor radius of the shell and the toroidal coil are 24 cm and 28 cm, respectively. The liner and the shell are, respectively, made of Inconel 625 and SUS 316. The time constant of the shell is 1 ms for vertical field penetration. The maximum discharge duration is 3 ms, with a plasma current of 250 kA. The current rise time is, typically, 0.5 ms. REPUTE-1 RFP is equipped with 54 single turn toroidal coils, which are connected in series (Fig. 1). Toroidal field ripple is calculated to be 1.5%. Here, the toroidal field ripple is defined as the ratio of the radial field at the plasma edge to the toroidal field at the plasma centre. Figure 2 shows plots of the calculated toroidal field ripple as a function of the number of toroidal field coils for various values of the pinch parameter. Here, the

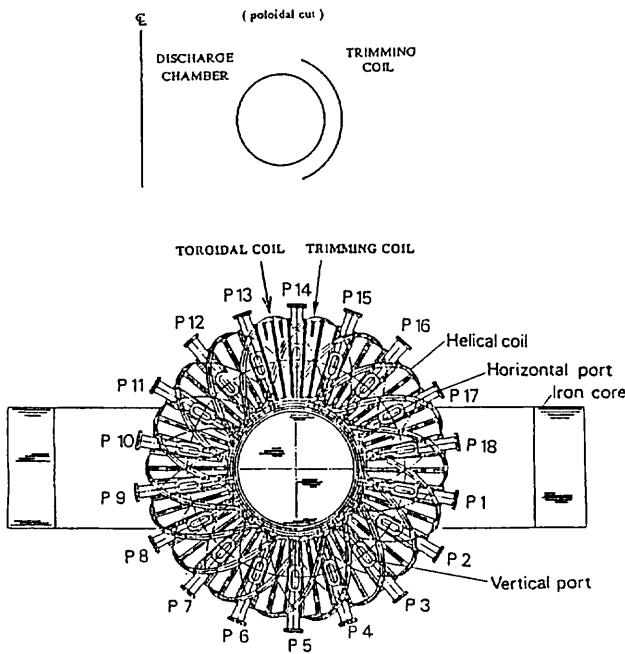


FIG. 1. Top view and poloidal cut of REPUTE-1 RFP. Toroidal coils and trimming coils for ripple reduction experiment in one section are indicated by arrows. Trimming coils are also provided in other sections (in the entire toroidal direction).

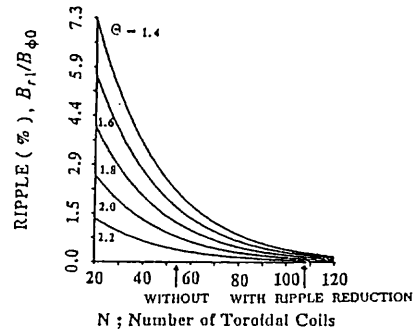
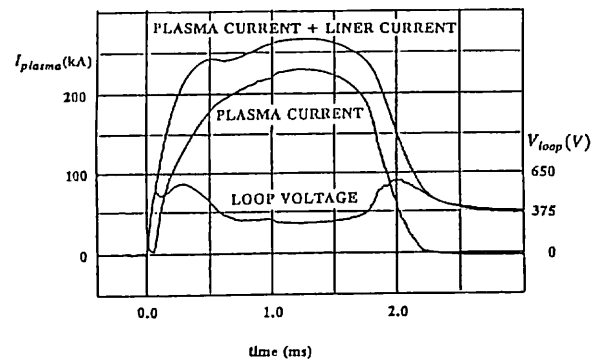


FIG. 2. Toroidal field ripple (theoretical value) as a function of number of toroidal coils. The ripple is defined as the ratio of the radial field at the plasma edge to the toroidal field at the plasma centre. (REPUTE-1 has 54 toroidal coils.)

(a) WITH RIPPLE REDUCTION



(b) WITHOUT RIPPLE REDUCTION

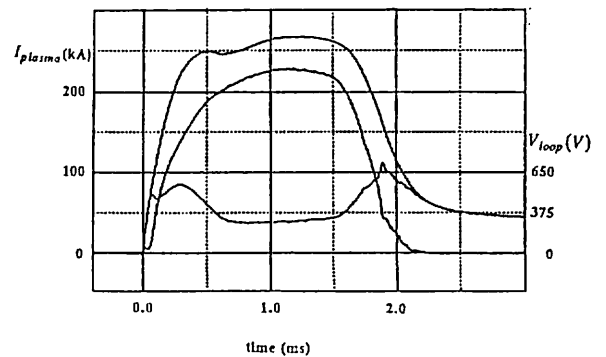


FIG. 3. Waveforms of global parameters for discharges with and without application of ripple reduction field. The ripple reduction field is applied after  $t = 1.0$  ms.

pinch parameter is defined as the ratio of the poloidal field at the wall to the volume averaged toroidal field. The calculation is made in cylindrical geometry, using the Bessel function model. To reduce the toroidal field ripple in the outer region of the plasma, a trimming coil subtending a poloidal arc of  $\pm 70^\circ$  relative to the mid-plane has been placed in the middle of the gaps between each pair of toroidal field coils (Fig. 1). These trimming coils are placed regularly all over the toroidal direction. The distance between the trimming coils and the minor axis of the discharge chamber is 30 cm. Trimming coils are activated by a 2 kV, 20 kJ capacitor bank switched by thyristors. The trimming coil current is set approximately equal to toroidal coil current. Then, we have a ripple of 0.3%, as a rough estimate, taking 108 for the number of toroidal coils (Fig. 2).

### 3. RESULTS

#### 3.1. Changes of global parameters

Error field reduction experiments making use of toroidal field trimming have led to a reduction of the loop voltage and, possibly, to an improvement in the

energy confinement and/or decrease of helicity dissipation at the plasma edge [9]. Figures 3(a) and (b) show typical discharge characteristics obtained in discharges with and without ripple reduction. In Fig. 3(a), the trimming field is applied 1 ms after plasma initiation, when the plasma is in the RFP configuration phase. After the application of the ripple reduction field, the toroidal loop voltage immediately decreases from 260 V to 230 V, and the toroidal plasma current increases from 220 kA to 230 kA. Accordingly, the plasma resistance decreases from 1.2 m $\Omega$  to 1.0 m $\Omega$ , and the corresponding electron conductivity temperature at the plasma centre increases from 60 eV to 70 eV. Here, we have assumed  $Z_{\text{eff}} = 2.0$ , helical factor = 8.0, plasma radius = liner radius = 22.0 cm, and a parabolic temperature profile. The Ohmic power input decreases by about 7%. We do not observe any substantial changes in other global parameters such as toroidal flux, toroidal field at the wall or line averaged electron density as measured by a CO<sub>2</sub> laser interferometer. Note that at this stage (end of 1987), other field errors, such as those arising from shell gaps, port holes and coil feeders, have not been reduced sufficiently. This might be a reason why the decrease in the loop voltage due to ripple reduction is not so large.

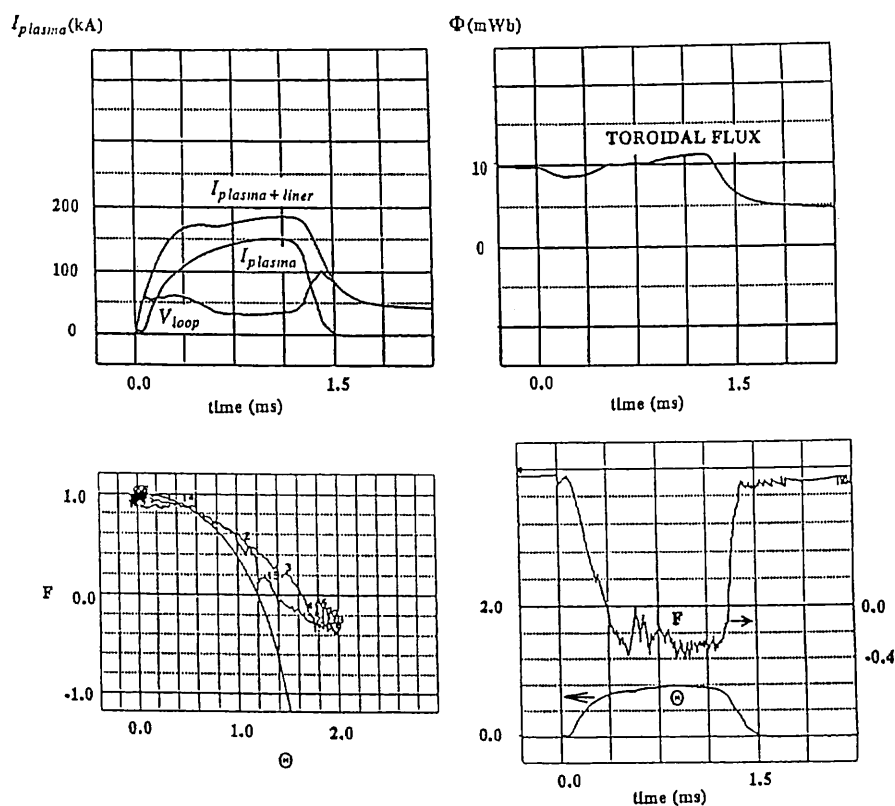
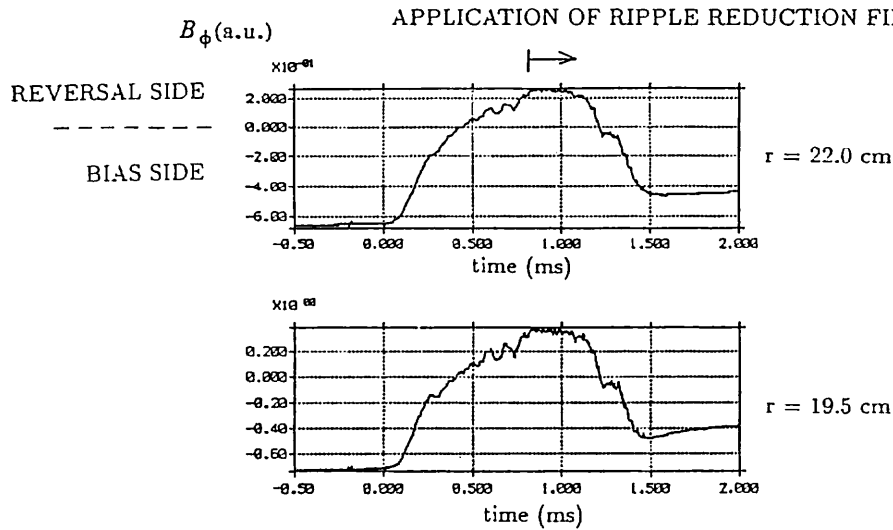


FIG. 4. Waveforms of global parameters of 150 kA discharge with probe inserted. After  $t = 0.8$  ms, the ripple reduction field is applied continuously.

## WITH RIPPLE REDUCTION



## WITHOUT RIPPLE REDUCTION

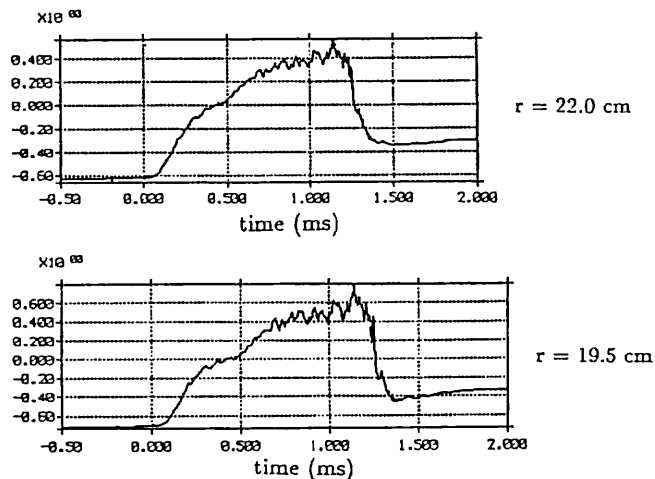


FIG. 5. Time evolution of toroidal fields inside plasma measured by inserted magnetic probe for discharges with and without ripple reduction field. Coil locations:  $r = 19.5$  cm and  $22.0$  cm.

### 3.2. Changes in magnetic field fluctuations

Changes in MHD fluctuations due to ripple reduction have been studied by measuring internal field fluctuations using an insertable magnetic probe for 150 kA discharges. An example for the loop voltage and current waveforms in these discharges is shown in Fig. 4, as well as the associated reversal ratio ( $F$ ), the pinch parameter ( $\Theta$ ), and the toroidal flux. The insertable probe has eight pairs of coils directed toroidally and poloidally and located every 2.5 cm from 4.5 cm to 22.0 cm in

the minor radius from the centre of the discharge chamber. The ripple reduction field is applied at  $t = 0.8$  ms. After this time, the loop voltage decreases from 205 to 195 V. Figure 5 shows the time history of the toroidal field measured by inserted probe coils located at  $r = 19.5$  cm and  $22.0$  cm, for discharges with and without ripple reduction field. A significant decrease in the fluctuations is observed for discharges with ripple reduction field. In contrast, the level of fluctuations for discharges without ripple reduction field never decreases.

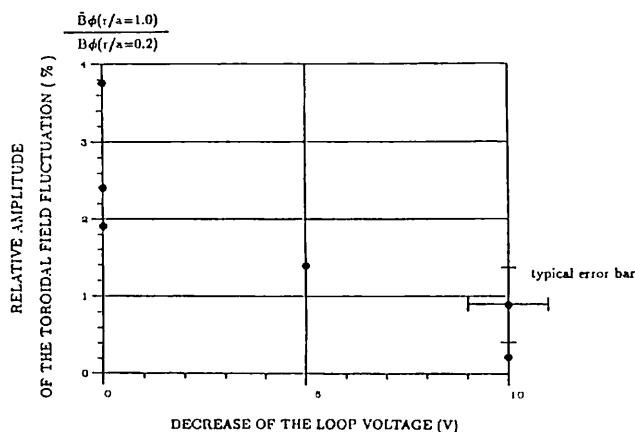


FIG. 6. Relation between relative toroidal field amplitude at liner radius and decrease in loop voltage due to ripple reduction. (Left hand points: discharges without ripple reduction; right hand points: discharges with ripple reduction field.)

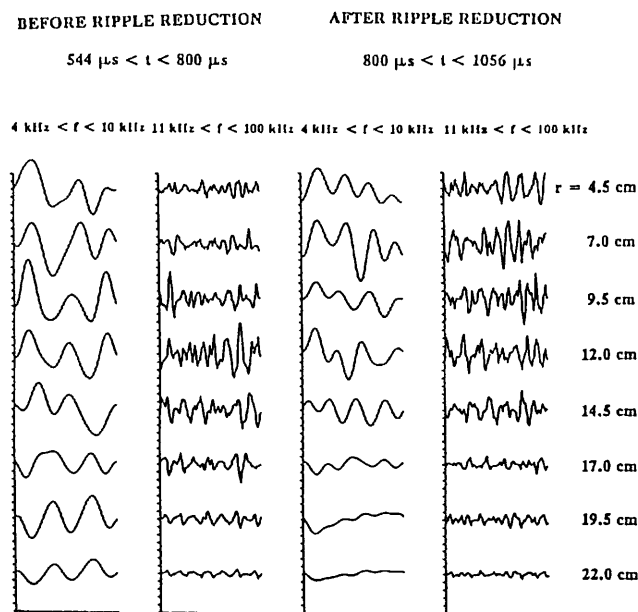


FIG. 7. Numerically filtered signals of toroidal field fluctuations for discharge with ripple reduction field.

Figure 6 shows the relationship between decreased loop voltage and relative amplitude of the toroidal field fluctuations at  $r = 22$  cm (liner radius), measured by an internal magnetic probe. The decrease in the loop voltage tends to become larger with decreasing relative amplitude of the fluctuations brought about by the application of the ripple reduction field.

A statistical analysis has been done for the field fluctuations. Here, we carry out calculations for two

different periods of a discharge, i.e. before and after application of the ripple reduction field, and compare the fluctuations during both periods. The first period is  $544 \mu\text{s} < t < 800 \mu\text{s}$ , and the second period is  $800 \mu\text{s} < t < 1056 \mu\text{s}$ . This method is sufficient to clarify the effect of the ripple reduction field, since little change is seen in the fluctuation character of two periods for the discharge without the ripple reduction field.

Signals are numerically filtered and divided into slow and fast fluctuations, i.e. a low band of  $4 \text{ kHz} < f < 10 \text{ kHz}$  and a high band of  $11 \text{ kHz} < f < 100 \text{ kHz}$ . The low band is of the order of one tenth of the toroidal Alfvén frequency, and the high band is of the order of the Alfvén frequency. Results are shown in Fig. 7. The slow fluctuations show strong coherence in space and time, while the fast fluctuations are only weakly coherent. At  $r = 22.0$  cm and  $19.5$  cm, a distinct decrease in the slow fluctuations is observed after application of the ripple reduction field whereas fluctuations of the high frequency part are not changed significantly.

The normalized time delayed cross-correlation function, to be defined below, provides quantitative understanding of the coherence in space and time:

$$\rho_{ij}(\tau) = \frac{\int_{t_0}^{t_0+T} x_i(t)x_j(t+\tau)dt}{\left\{ \int_{t_0}^{t_0+T} x_i(t)^2 dt \int_{t_0}^{t_0+T} x_j(t+\tau)^2 dt \right\}^{1/2}}$$

where  $x_i(t)$  denotes the signal of the  $i$ -th channel. The integral time length  $T$  is  $80 \mu\text{s}$  for the low band and  $16 \mu\text{s}$  for the high band. The delay time  $\tau$  lies in the range  $(-40 \mu\text{s}, +40 \mu\text{s})$ . The reference signal is the one measured at  $r = 17$  cm, which approximately corresponds to the position of the reversal surface. In Figs 8(a) and (b) we see a significant change, caused by the ripple reduction, in the cross-correlation function of the low band. Before the ripple reduction, the signals of the outer two channels are well correlated (Fig. 8(a)). After the ripple reduction, the cross-correlation function of the outer two channels becomes nearly zero for almost the entire delay time. This shows the stabilization of the coherent MHD instability. In contrast, the cross-correlation functions of the high band are small and insensitive to the ripple reduction field (Figs 8(c) and (d)).

The reproducibility of the tendency observed above is checked by Fig. 9, which shows traces of the zero time delay cross-correlation function for four discharges

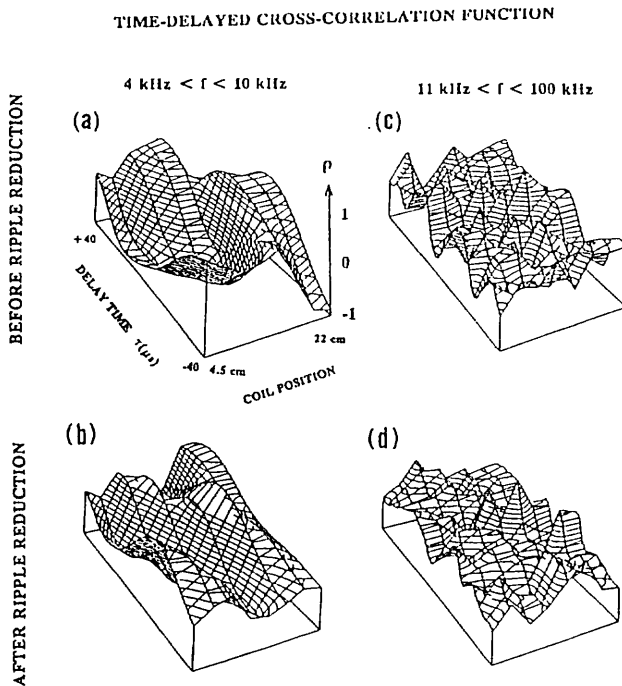


FIG. 8. Normalized cross-correlation function of the signals of Fig. 6. Reference channel located at  $r = 17.5$  cm. (a)  $4 \text{ kHz} < f < 10 \text{ kHz}$ , before the application of the ripple reduction field; (b)  $4 \text{ kHz} < f < 10 \text{ kHz}$ , after application; (c)  $11 \text{ kHz} < f < 100 \text{ kHz}$ , before application; (d)  $11 \text{ kHz} < f < 100 \text{ kHz}$ , after application.

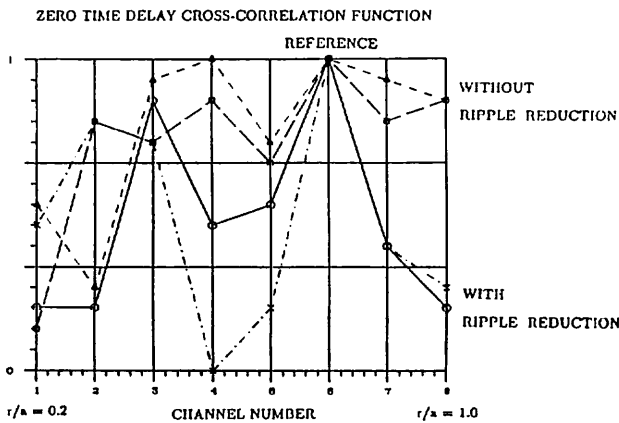


FIG. 9. Traces of zero time delay cross-correlation function for four discharges with/without ripple reduction.

with/without ripple reduction field. Near the plasma centre, it is hard to distinguish the characters of the discharges with and without ripple reduction field. Near the plasma edge, however, the decrease in the cross-correlation function due to the application of the ripple reduction field is remarkable.

We now discuss the mode structure of the MHD fluctuations. The slow and coherent fluctuations of the toroidal fields are considered to be a manifestation of the  $m = 1$  kink mode. Figures 10(a) and (b) show the radial structures of the internal toroidal and poloidal magnetic field fluctuations normalized by the zero order toroidal field at  $r = 2.5$  cm. Their calculated [10] and observed [11, 12] eigenfunctions of the  $m = 1$  mode are similar in that they have opposite signs at the inner

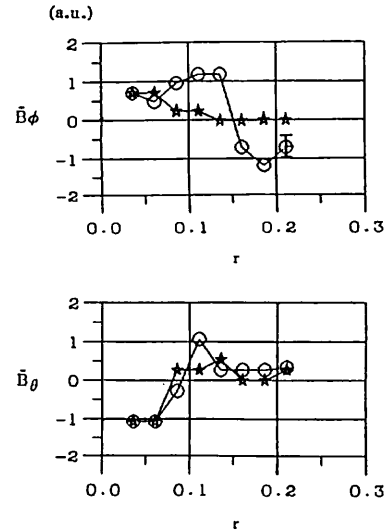


FIG. 10. Spatial structure of toroidal and poloidal field perturbations for discharges with (stars) and without (circles) ripple reduction.

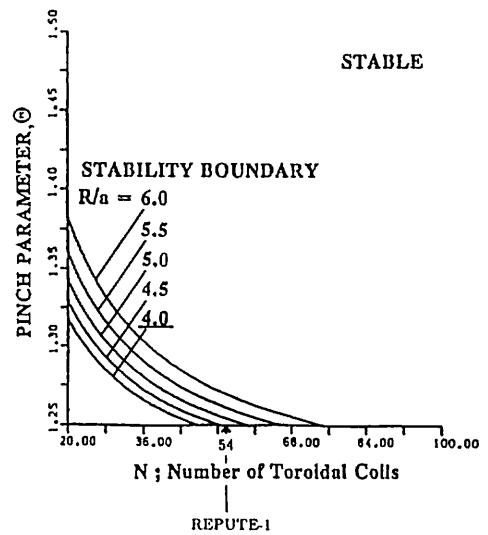


FIG. 11. Stability diagram of  $m = 0$  tearing mode in  $\Theta - N$  space for REPUTE-1 RFP geometry. The conducting wall lies at infinity in the calculation in order to simulate the thin shell condition of the device.

and the outer part of the plasma and the poloidal field perturbation has a finite value near the plasma centre. The  $m = 0$  component is considered to be negligible since the amplitude of the poloidal field perturbation has a finite value near the plasma centre. This consideration is confirmed by  $m = 0$  tearing mode analysis which treats the toroidal field ripple [5]. Figure 11 shows a stability diagram of the  $m = 0$  tearing mode in  $\Theta$ - $N$  space for REPUTE-1 geometry, where  $\Theta$  is a pinch parameter and  $N$  is the total number of toroidal coils. In the calculation, the Bessel function model is used as a magnetic field profile in cylindrical approximation, and the plasma response is included. The  $m = 0$  mode is stable above the curve. Figure 8 shows that the REPUTE-1 RFP plasma is in the stable regime for the  $m = 0$  tearing mode, even without the trimming field. The mode whose poloidal mode number is above 1 is less important for the stability analysis [10].

#### 4. SUMMARY AND DISCUSSION

The toroidal field ripple reduction experiment on REPUTE-1 has demonstrated stabilization of coherent MHD activities (possibly the  $m = 1$  mode) and a consequent decrease in the loop voltage. The decrease in the loop voltage is supposed to be brought about by the decrease in the plasma resistance itself and/or by the decrease in helicity dissipation in the edge region. It is difficult to determine the balance of these two effects since the electron temperature is not measured and the size of the vacuum region is hard to determine. The decrease of the edge region is, however, estimated to be around 1 cm in minor radius when the decrease of the loop voltage is assumed to be only due to the decrease in helicity dissipation, on the assumption that the electric field is parallel to the magnetic field,  $E_{\parallel} \approx 30 \text{ V} \cdot \text{m}^{-1}$  [9]. A more detailed discussion needs further quantitative measurements.

The stabilization of the  $m = 1$  kink mode is considered to be due to the change in the equilibrium (or zero order) field given by the ripple reduction and also by the reduction of the kink activities themselves. It is worth while noting that the  $m = 1$  activities are strongly affected by an  $m = 0$  perturbation of the ripple reduction field. The kink mode with  $m = 1$  has been shown to be more easily destabilized by a smaller toroidal field ripple. We had to improve the toroidal field ripple down to 0.3% (theoretical estimate) to bring about a significant stabilization of  $m = 1$  kink activities.

#### REFERENCES

- [1] BODIN, H.A.B., NEWTON, A.A., Nucl. Fusion 20 (1980) 1255.
- [2] MASSEY, R.S., MILLER, G., BUCHENAUER, C.J., MOSES, R.W., BURKHARDT, L.C., SCHOENBUERG, K.F., JACOBSON, A.R., WATT, R.G., MELTON, J.G., Equilibrium and Error Field Study on ZT-40, Rep. LA-9567-MS, Los Alamos National Laboratory, NM (1983).
- [3] HOWELL, R.B., VOGEL, H.F., J. Appl. Phys. 56 (1984) 2017.
- [4] MILLER, G., Phys. Fluids 28 (1985) 560.
- [5] PINSKER, R.I., REIMAN, A.H., Phys. Fluids 29 (1986) 782.
- [6] NOONAN, P.G., TSUI, H., NEWTON, A.A., Plasma Phys. Contr. Fusion 17 (1985) 1307.
- [7] SHIMADA, T., HIRANO, Y., YAGI, Y., NEWTON, A.A., OGAWA, K., in Plasma Physics and Controlled Nuclear Fusion Research 1986 (Proc. 11th Int. Conf. Kyoto, 1986), Vol. 2, IAEA, Vienna (1987) 453.
- [8] MIYAMOTO, K., INOUE, N., Nucl. Fusion 25 (1985) 1303.
- [9] JARBOE, T., ALPER, B., Phys. Fluids 30 (1987) 1177.
- [10] ROBINSON, D.C., Nucl. Fusion 18 (1978) 939.
- [11] TAMANO, T., CARLSTROM, T., CHU, C., et al., in Plasma Physics and Controlled Nuclear Fusion Research, 1982 (Proc. 9th Int. Conf. Baltimore, 1982), Vol. 1, IAEA, Vienna (1983) 609.
- [12] BROTHERTON-RATCLIFFE, D., GIMBLETT, C., HUTCHINSON, I., Plasma Phys. Contr. Fusion 29 (1987) 161.

(Manuscript received 2 April 1987)

Final manuscript received 8 October 1987)